

Neuro-fuzzy based prediction of the durability of self-consolidating concrete to various sodium sulfate exposure regimes

M. T. Bassuoni

*School of Planning, Architecture and Civil Engineering
Centre for Built Environment Research, Queen's University of Belfast, Belfast BT9 5AG, UK*

M. L. Nehdi*

*Department of Civil and Environmental Engineering, The University of Western Ontario
London, Ontario N6A 5B9, Canada*

(Received March 13, 2008, Accepted October 23, 2008)

Abstract. Among artificial intelligence-based computational techniques, adaptive neuro-fuzzy inference systems (ANFIS) are particularly suitable for modelling complex systems with known input-output data sets. Such systems can be efficient in modelling non-linear, complex and ambiguous behaviour of cement-based materials undergoing single, dual or multiple damage factors of different forms (chemical, physical and structural). Due to the well-known complexity of sulfate attack on cement-based materials, the current work investigates the use of ANFIS to model the behaviour of a wide range of self-consolidating concrete (SCC) mixture designs under various high-concentration sodium sulfate exposure regimes including full immersion, wetting-drying, partial immersion, freezing-thawing, and cyclic cold-hot conditions with or without sustained flexural loading. Three ANFIS models have been developed to predict the expansion, reduction in elastic dynamic modulus, and starting time of failure of the tested SCC specimens under the various high-concentration sodium sulfate exposure regimes. A fuzzy inference system was also developed to predict the level of aggression of environmental conditions associated with very severe sodium sulfate attack based on temperature, relative humidity and degree of wetting-drying. The results show that predictions of the ANFIS and fuzzy inference systems were rational and accurate, with errors not exceeding 5%. Sensitivity analyses showed that the trends of results given by the models had good agreement with actual experimental results and with thermal, mineralogical and micro-analytical studies.

Keywords: Neuro-fuzzy systems; self-consolidating concrete; sulfate attack; environmental conditions; flexural loading.

1. Introduction

Fuzzy inference systems (FIS) are modelling tools that can handle ambiguity and errors in complex systems. System components are mapped (fuzzified) to partial degrees of belongings of membership functions. All non-linear and complex relations between system components are handled using linguistic rules in the form of IF-THEN statements in rule-based engines to convert

* Corresponding Author, E-mail: mnehdi@eng.uwo.ca

fuzzified inputs (antecedents) to fuzzy outputs (consequents). Outputs of respective rules are aggregated and defuzzified to give a scalar solution. Extensive details on FIS and its mathematics are beyond the scope of this paper and are given by Ross (2004). Several investigations used FIS to study various durability aspects of concrete. For instance, Do, *et al.* (2005) developed a fuzzy arithmetic approach to rationally estimate the time-to-corrosion initiation for reinforced concrete elements exposed to chlorides. Anoop, *et al.* (2002) and Do (2006) used FIS to determine the effects of environmental conditions accompanying chloride-rich environments on estimating the service life of reinforced concrete structural members and their cover thickness, respectively. Also, Kim, *et al.* (2006) has introduced a fuzzy-based assessment system for reinforced concrete structures to efficiently estimate their current state and present a guide for future maintenance and management.

Artificial neural networks (ANNs) are another artificial intelligence-based computational tool capable of pattern recognition and self-learning. The basic operations of such systems simulate that of neurons of the human brain (El-Chabib and Nehdi, 2005). ANNs usually consist of input, hidden and output layers that comprise neurons (processing units). Neurons of one layer are partially or fully connected to neurons in the succeeding layer, but are not connected to conjugate neurons in the same layer. Such a type of networks is classified as feed-forward ANNs. A large number of data is usually needed to train ANNs in order to learn relationships between input parameters and their corresponding outputs. In ANNs, the back-propagation technique is commonly used for training ANNs where the convergence of ANNs is determined based on minimizing least-square calculations between the output of the network and their corresponding actual values. Accordingly, the weights (strength of connections) between connected neurons are continually updated until the global error (usually the root mean-squared error, RMSE) reaches a desired minimum value or the number of epochs (training patterns) reaches a designated value. Substantial information on ANNs is available in the open literature (e.g. Haykin 1999). Recently, El-Chabib and Nehdi (2005) thoroughly explained the application of ANNs to model the properties of cement-based materials. Several investigators used ANNs to accurately predict the deterioration in engineering properties of cement-based materials exposed to aggressive conditions. For example, Haj-Ali, *et al.* (2001) and Göktepe, *et al.* (2006) showed the capability of ANNs to reasonably estimate the expansion of concretes/mortars exposed to sulfate solutions based on parameters such as w/cm and C₃A content in the cementitious system.

Adaptive neuro-fuzzy inference systems (ANFIS) are effective in modelling scenarios of known input-output data of complex systems. They possess the learning capabilities of ANNs and accommodate uncertainty/errors and interference of human approximation, which are the inherent advantages of FIS (Brown and Harris, 1994). This helps tailoring the membership functions of FIS to variation in given input-output data sets. In ANFIS, the FIS learn information about data to compute parameters of membership functions that best describe input-output behaviour. The algorithm works similarly to that of ANNs. The learning process is initiated by generating parameters associated with input membership functions (antecedents). Parameters associated with output membership functions (consequents) are computed to satisfy a minimum RMSE. The parameters of antecedents are then updated using a back-propagation technique from which the new parameters of consequents are recomputed. Thus, the rule-based engine (antecedents and consequents) is dynamically updated. The process continues until a global minimum RMSE or a designated number of epochs is reached (Brown and Harris 1994, Ross 2004). A proposed ANFIS architecture is trained and tested using an appropriate database, which should ideally cover the controlling parameters of output variables.

Using a well-defined experimental database, ANFIS can be an efficient tool in modeling complex durability issues such as chloride induced corrosion, alkali aggregate reaction and sulfate attack of concrete as shown by recent investigations. ANFIS has feasibly been used to develop building management systems that are capable of analyzing the condition state of reinforced concrete structures under severe conditions of environment and loading (Kawamura and Miyamoto 2003). Ming-yu and Ming-shu (2006) have successfully applied ANFIS to evaluate the effect of composition (contents of CaO, Na₂O and K₂O) of fly ash on suppressing the expansion of concrete due alkali aggregate reaction. More recently, İnan, *et al.* (2007) have introduced an ANFIS model based on grid partitioning to predict the expansion of mortar specimens in a standard sulfate evaluation test (ASTM C 1012). The selected input parameters for the model were C₃A content, C₃S/C₂S ratio, solution concentration, and mineral admixture substitution level (İnan, *et al.* 2007).

The deterioration mechanisms of cement-based materials due to external sulfate attack depend on multiple factors such as constituent materials, environmental conditions, type of cation, etc. Substantial information on this complex durability issue can be found in the open literature (e.g. Cohen and Mather 1991, Hewlett 1998, Mehta 2000, Al-Amoudi 2002, Skalny, *et al.* 2002, Neville 2004). The ACI 201.2R Guide to Durable Concrete provides useful guidelines on improving the resistance of cement-based materials to various exposure classes of sulfate attack (2001). Despite the available knowledge on sulfate attack of cement-based materials, there are still conflicting theories (Brown and Taylor 1999) and ill-defined degradation mechanisms (Skalny and Pierce 1999, Neville 2004). Currently available computer models of external sulfate attack of concrete such as CONCLIFE (Bentz, *et al.* 2001 and Ferraris, *et al.* 2006) and STADIUM (Marchand, 2001 and Samson and Marchand 2007) give useful predictions on the deterioration of concrete. CONCLIFE predicts the service life of concrete based on the critical thickness of spalled concrete, while STADIUM predicts the sulfate and solid phase (ettringite, gypsum, etc.) distributions in concrete under sulfate attack. However, both models are deterministic in nature without providing any information on the deterioration of concrete in terms of physico-mechanical properties (e.g. expansion and loss of strength), which are important manifestations of damage due to sulfate attack.

A complex phenomenon such as external sulfate attack of cement-based materials involves ambiguous/unknown relationships between sulfate attack mechanisms of deterioration, concrete mixture proportions, environmental exposure conditions, structural loading and the selected criteria of evaluation (e.g. expansion). Thus, it should be modeled considering uncertainty, non-linearity and interface of multiple factors. Based on the promising use of artificial intelligence techniques in modelling complex durability issues of concrete as indicated by the literature, the present study aims at predicting the expansion, relative elastic dynamic modulus (RE_d) and the time of failure (TF) for a variable range of self-consolidating concrete (SCC) mixture designs under various sulfate attack exposure regimes using ANFIS. Three ANFIS models were developed, trained and tested using experimental data from a comprehensive testing program conducted at the University of Western Ontario. In addition, a fuzzy inference system was developed to forecast the level of aggression of environmental conditions associated with sulfate attack by an environmental impact factor (EIF).

The resistance of SCC to external sulfate attack is linked to its microstructure and particular mixture design variables (e.g. composite cements with a larger volume fraction of supplementary cementitious materials [SCMs]). The larger powder content (400-600 kg/m³) and volume of cementitious paste (34-40%) of SCC (ACI 237R, 2007) can make it particularly vulnerable to chemical attack, for example by sulfate solutions. SCC has been progressively used in chemically vulnerable areas such as sewage, substructures, pavements, industrial floors, etc. While many of

these applications are susceptible to external sulfate attack, only few studies investigating the resistance of SCC to sulfate attack have been reported in the open literature (RILEM TC 205-DSC, 2007, Bassuoni 2008). According to Boel, *et al.* (2007) and Zhu and Bartos (2003) essential knowledge on the durability of SCC is still needed before its safe use in various applications. Therefore, a comprehensive program was conducted at the University of Western Ontario to provide fundamental knowledge on the resistance of a wide scope SCC mixture designs to external sulfate attack. The current work describes the modeling part of this program. Full details on the experimental part of this program are beyond the scope of the current study and can be found in Bassuoni (2008).

2. Experimental program

2.1. Materials

Twenty one SCC mixtures with a w/cm of 0.38 were prepared using single, binary, ternary and quaternary binders. The mixtures were divided into three groups: Group A (non-air-entrained SCC with a sand-to-total aggregates mass ratio [S/A] of 50%); Group B (air-entrained SCC mixtures with S/A of 40 and 60%); and Group C (air-entrained SCC with fibre reinforcement and sand-to-total aggregates plus fibres mass ratio of 50%). The binders used included CSA Type 10 (ASTM Type I) ordinary portland cement (OPC), CSA Type 50 (ASTM Type V) sulfate resistant portland cement (SRPC), silica fume (SF), Class F fly ash (FA), slag (S), and limestone filler (LF). Details of the chemical and physical properties of the various binders are listed in Table 1. Single binders were

Table 1 Chemical and physical properties of cement and SCMs

	OPC	SRPC	Silica Fume	Fly Ash	Slag	Limestone Filler
SiO ₂ (%)	19.8	22.3	94.0	48.9	35.0	0.3
CaO (%)	63.2	63.8	0.4	3.8	36.1	--
Al ₂ O ₃ (%)	5.0	3.5	0.1	23.3	11.2	--
Fe ₂ O ₃ (%)	2.4	4.0	0.1	14.9	0.5	--
MgO (%)	3.3	2.8	0.4	0.7	11.4	--
K ₂ O (%)	1.2	0.4	0.9	1.7	0.5	--
SO ₃ (%)	3.0	2.1	1.3	0.2	3.3	--
Na ₂ O (%)	0.1	0.1	0.1	0.6	0.5	--
TiO ₂ (%)	0.3	--	0.3	--	0.6	--
CaCO ₃ (%)	--	--	--	--	--	99.0
Loss on ignition (%)	2.5	0.9	4.7	0.3	--	--
Specific surface area (m ² /kg)	410	377	19530	280	468	3200
Specific gravity	3.17	3.15	2.12	2.08	2.90	2.70
C ₃ S	61	54	--	--	--	--
C ₂ S	11	23	--	--	--	--
C ₃ A	9	1	--	--	--	--
C ₄ AF	7	14	--	--	--	--

100% OPC (control) or 100% SRPC, binary binders contained 92% OPC and 8% SF, and ternary binders contained 50% OPC, 5% SF and 45% S. Quaternary binders comprised 50% OPC, 15% LF, 20% S and 15% FA, or 50% OPC, 5% SF, 25% S and 20% FA.

The fine aggregate was natural siliceous sand with a fineness modulus of 2.80, a saturated surface dry specific gravity of 2.65 and water absorption of 1.5%. Crushed stone (mostly siliceous gravel with a fraction of limestone aggregate) with a maximum nominal size of 19 mm, a saturated surface dry specific gravity of 2.68 and water absorption of 0.8% was also used. A polycarboxylate-based high-range water-reducing admixture (HRWRA) and a viscosity-modifying admixture (VMA) based on a solution of modified polysaccharide were used to enhance the flowability and stability of the SCC mixtures. The dosages of HRWRA and VMA were adjusted to maintain a slump flow of 650 ± 30 mm and L-box (3Ø10 mm bars with 50 mm gaps) ratio (H_2/H_1) not less than 0.70 for all mixtures. A multi-component synthetic air-entraining admixture (AEA) was used in groups B and C mixtures to obtain a fresh air content of 4-7%.

In group C mixtures, micro-reinforcement of polypropylene fibrillated fibres with a specific gravity of 0.91 and graded length were added at a single dosage of 0.1% by volume. In addition, macro-reinforcement of crimped steel fibres with a specific gravity of 7.85, length of 38 mm, aspect ratio of 34, and tensile strength of 966-1242 MPa were used at a dosage of 0.4% by volume. Based on trial mixtures, these fibre shapes, lengths, and low volumes of micro- and macro-fibre reinforcement have proven adequate for achieving the characteristic flowability and passing ability of SCC with minimal clustering of fibres.

2.2. Experimental procedures

Constituent materials were mixed in a mechanical mixer in accordance to ASTM C 192 (Standard Practice for Making and Curing Concrete Test Specimens in the Laboratory). Tables 2a-b show the proportions of the tested SCC mixtures. Replicates of 75×150 mm concrete cylinders and 75×75×285 mm concrete prisms were prepared without compaction for the different tests. All specimens were demolded after 24 hours and moist cured at 20°C and 95% RH for 56 days. To evaluate the durability of the tested SCC mixtures to very severe sodium sulfate attack, five exposure regimes were adopted:

Exposure I: A reference exposure similar to that for ASTM C 1012 (2004) (Standard Test Method for Length Change of Hydraulic-Cement Mortars Exposed to a Sulfate Solution) in which prismatic SCC specimens were fully immersed in a 5% sodium sulfate solution for up to 24 months. The temperature of the solution was maintained at around $22 \pm 2^\circ\text{C}$. The solution was renewed each 18 weeks, and the pH was controlled at a range of 6.0-8.0 by titration with diluted sulfuric acid solutions at regular time intervals (5 days). While controlling the pH of the sulfate solution was not specified in the ASTM C 1012, the importance of a controlled pH (6.0-8.0) of the sulfate solution correlates to field conditions in which concrete exists in a neutral environment with continual supply of sulfate ions (Skalny, *et al.* 2002).

Exposure II: A wetting-drying exposure in which prismatic concrete specimens were subjected to a sulfate solution and drying in hot environment. A wetting-drying cycle consisted of four days of full immersion in a 5% sodium sulfate solution and three days of drying at 45°C and 35% RH in an environmental chamber. This exposure continued for up to 24 months (104 cycles). Renewal of solutions and pH control were conducted in a similar way to exposure I.

Exposure III: A wetting-drying exposure in which cylindrical concrete specimens were subjected

to partial immersion in a sulfate solution and drying in hot environment. One cycle consisted of partial immersion (to a depth of 50 mm) in a 5% sodium sulfate solution for four days during which the top two-thirds (100 mm) of each specimens were exposed to drying under $22\pm 2^\circ\text{C}$ and $55\pm 5\%$ RH. Then, the entire cylindrical specimens were submitted to drying under 45°C and 35% RH for three days. The experiment lasted for 24 months (104 cycles), and renewal of solutions and pH control were done similar to the above two exposure regimes.

Exposure IV: A freezing-thawing exposure which involved concomitant chemical and physical attack by sodium sulfate and freezing-thawing cycles. Prismatic SCC specimens were fully immersed for 2 days in a 5% sodium sulfate solution followed by 2 days of freezing in air at -18°C . After 365 days (approximately 90 freezing-thawing cycles), the procedure was accelerated. Specimens were subjected to successive freezing-thawing cycles interrupted by wetting and drying periods. A full exposure cycle consisted of 5 days of immersion in 5% sodium sulfate solution at 20°C , 5 days (26 freezing-thawing cycles) in an automated freezing-thawing cabinet adjusted to the ASTM C 666 procedure A (Standard Test Method for Resistance of Concrete to Rapid Freezing and Thawing in Water) (2004) except that a 5% sodium sulfate solution was used instead of water, and 2 days of drying at 20°C and 50% RH. Subsequent to the initial 90 freezing-thawing cycles, the number of accelerated cycles for specimens from groups A, B and C were selected to be 10, 15 and 20 cycles, respectively. This is equivalent to 350, 480, and 610 freezing-thawing cycles, respectively. Replacement of solutions and pH control was done similar to the previously described exposure regimes.

Exposure V: In this exposure, SCC specimens from the same mixtures were subjected to multiple damages of sodium sulfate, cyclic environmental conditions and sustained flexural loading. Prismatic SCC specimens were subjected to stress ratios of 25 and 50% of their ultimate flexural strength. Flexural stress was mechanically applied to the specimens in four-point bending and sustained using steel frames with dual springs. These stress levels were maintained till the end of exposure. Comparatively, companion specimens were exposed to sulfate attack and cyclic environmental conditions without flexural stress.

Specimens with and without sustained flexural stress were initially immersed for 5 days in a 5% sodium sulfate solution (pH 6.0-8.0) at a temperature of $20\pm 2^\circ\text{C}$ before being exposed to the cyclic environmental conditions that simulated successive winter and summer seasons. A winter season was represented by 30 successive freezing-thawing cycles: freezing in air at $-18\pm 1^\circ\text{C}$ for 12 hours followed by thawing in a 5% sodium sulfate solution (pH 6.0-8.0) at $5\pm 1^\circ\text{C}$ for 6 hours, and 4 hours to ramp to the minimum freezing temperature and 2 hours to ramp to the maximum thawing temperature. A summer season comprised 8 alternating wetting-drying cycles. Each cycle consisted of 2 days of immersion in a 5% sodium sulfate solution (pH 6.0-8.0) at a temperature of $22\pm 2^\circ\text{C}$ followed by 2 days of drying at 40°C and 40% RH. The experiment was conducted in a state-of-the-art walk-in environmental chamber with programmable and automated temperature and RH controls. The solution was renewed every 30 days (season) and pH control was done similar to that for the reference exposure. The experiment lasted for one year, simulating 6 winters alternating with 6 summers under sustained flexural loading and sulfate attack.

Before any exposure, the initial physico-mechanical properties of the intact specimens were determined. The initial length (ASTM C 1012) and dynamic modulus of elasticity, E_d (ASTM C 215 (2004) Standard Test Method for Fundamental Transverse Resonant Frequency of Concrete Specimens, calculated as the square of the fundamental transverse frequency according to the ASTM C 666 guidelines) were recorded. Specimens were removed from the sulfate solutions at specified time intervals for regular evaluation. Relative to the initial values, the change in length

and dynamic modulus of elasticity (RE_d) versus time of exposure were calculated. The starting time of failure (TF) of SCC specimens was determined based on an increase in expansion beyond 0.1%, and/or a decline in RE_d below 60%, or breakage of specimens by transverse macro-cracks.

To analyze the characteristics of the pore structure, mercury intrusion porosimetry (MIP) was conducted on specimens from the tested binders. To analyse the sulfate reaction phases, differential scanning calorimetry (DSC) was conducted on powder samples collected from the surface of selected specimens. To complement the results obtained by DSC, X-ray diffraction (XRD, Cu-K α) was conducted on similar powder samples. To assess the deterioration of the microstructure, polished sections were prepared for optical microscopy. Backscattered and secondary scanning electron microscopy (BSEM, SEM) with energy dispersive X-ray analysis (EDX) were also conducted on selected thin sections and fracture surfaces to supplement the findings of optical microscopy. Details of these studies (Bassuoni 2008) are beyond the scope of the current work. However, some observations of these studies are introduced in the discussion of models' predictions to explain significant trends in the results and validate the models' predictions with direct experimental evidence.

3. Anfis models

3.1. Database

To investigate the resistance of a wide range of SCC mixtures to sulfate attack, different types of cementitious binders (single, binary, ternary and quaternary) comprising OPC, SRPC, SF, FA, S and LF were tested. Other mixture design variables included air-entrainment, sand-to-aggregate ratio and hybrid fibre (steel and polypropylene) reinforcement. As explained above, specimens from the SCC mixtures were exposed to combined environmental and mechanical loading conditions along with very severe sodium sulfate attack. The expansion, deterioration of elastic dynamic modulus relative to its initial values (RE_d), and the time at which failure started (time of failure, TF) were determined for all test specimens.

Model I was developed to predict the free expansion of SCC specimens exposed to various high-concentration sodium sulfate exposure regimes. The database for training and testing this model contained 168 data points from 21 SCC mixtures (Table 2) that were exposed to high-concentration

Table 2a Proportions of binders per cubic meter of concrete

Binder Description	Binder Code	Cement kg, (lb)	Silica Fume kg, (lb)	Slag kg, (lb)	Fly Ash kg, (lb)	Lime-stone kg, (lb)
100% OPC	A1, B1 or C1	470	--	--	--	--
100% SRPC	SRPC	470	--	--	--	--
92% OPC, 8% SF	A2, B2 or C2	430	40	--	--	--
50% OPC, 5% SF, 45% S	A3, B3 or C3	235	25	210	--	--
50% OPC, 15% LF, 20% S, 15% FA	A4, B4 or C4	235	--	95	70	70
50% OPC, 5% SF, 25% S, 20% FA	A5, B5 or C5	235	25	120	90	--

OPC: ordinary portland cement; SRPC: sulfate resistant portland cement; SF: silica fume; S: slag; LF: lime-stone filler; FA: fly ash

sodium sulfate attack under four exposure regimes (full immersion, wetting-drying, freezing-thawing, and cyclic cold-hot conditions without sustained flexural loading). The model and database had eleven input variables: contents of OPC, SRPC, SF, S, FA, LF, sand, gravel, air, hybrid fibres and code of environmental exposure. This code was arbitrarily assigned with numbers from 1 to 4 to designate the sequence of experiments (Table 3). Such coding does not implicate the weight or aggression level of a specific exposure. Expansion of SCC specimens was the measured experimental parameter in the database and hence the predicted output of the model. The database of expansion was randomly divided into 138 and 30 data sets for training and testing, respectively. The properties of the training and testing data for Model I are listed in Table 4.

Model II was developed to predict the relative dynamic modulus of elasticity (RE_d) of SCC specimens under various high-concentration sodium sulfate exposure regimes. The database for training and testing Model II comprised 294 data points from 21 SCC mixtures that were exposed

Table 2b Proportions of groups A, B and C mixtures per cubic meter of concrete

Binder Code	Mix. ID	Steel Fibres (kg)	Polypropylene Fibres (kg)	Fine Aggregate (Kg)	Coarse Aggre- gate (kg)	Air-Entraining Agent (ml/100 kg of binder)
Group A						
SRPC	SRPC	--	--	870	870	--
A1	A1-N-50	--	--	870	870	--
A2	A2-N-50	--	--	860	860	--
A3	A3-N-50	--	--	855	855	--
A4	A4-N-50	--	--	845	845	--
A5	A5-N-50	--	--	840	840	--
Group B						
B1	B1-A-40	--	--	655	1015	45
	B1-A-60	--	--	1015	655	35
B2	B2-A-40	--	--	640	990	70
	B2-A-60	--	--	990	640	50
B3	B3-A-40	--	--	640	985	70
	B3-A-60	--	--	985	640	60
B4	B4-A-40	--	--	625	970	110
	B4-A-60	--	--	970	625	95
B5	B5-A-40	--	--	625	965	120
	B5-A-60	--	--	965	625	100
Group C						
C1	C1-A-H	30	1	830	805	40
C2	C2-A-H	30	1	825	795	60
C3	C3-A-H	30	1	820	790	65
C4	C4-A-H	30	1	805	780	100
C5	C5-A-H	30	1	800	775	105

Table 3 Coding of sulfate attack exposure regimes

Description of Exposure	Designated Code	
	Model I	Models II & III
Full Immersion	1	1
Wetting-Drying	2	2
Partial Immersion	--	3
Freezing-Thawing	3	4
Cyclic Cold-Hot Conditions	4	5

Table 4 Range of training and testing output variables for models I, II and III

Model/Property	Training Data			Testing Data		
	Min.	Max.	Avg.	Min.	Max.	Avg.
I/Expansion (%)	0.010	0.630	0.136	0.011	0.632	0.152
II/ RE_d (%)	0.0	118.0	73.0	0.0	114.0	71.7
III/ TF (Days)	21	728	491	30	728	451

to high-concentration sodium sulfate attack under five exposure regimes (full immersion, wetting-drying, partial immersion, freezing-thawing, and cyclic cold-hot conditions without and with sustained flexural loading). The model and database had an additional parameter (accounting for the flexural stress ratio) to the eleven variables previously described in the database of Model I. Thus, Model II and the associated database had a total of twelve input variables. The coding of the environmental exposure was similar to that of Model I database, except that the designated numbers varied from 1 to 5 (Table 3). Again, this arbitrary coding expressed the sequence of experiments and not the level of aggression of exposure. RE_d of SCC specimens was the experimental result in the database and hence the output of the predictive Model II. The database of Model II was randomly divided into 244 and 50 data sets for training and testing, respectively. The properties of the training and testing data sets for Model II are listed in Table 4.

Model III was developed to predict the time of initiation of failure (TF) of SCC specimens under various high-concentration sodium sulfate exposure regimes. The database for training and testing Model III comprised 294 data points. The database of Model III was identical to that of Model II, but TF of the SCC specimens was the experimental result in the database and hence the output of the predictive model III. The database of TF was randomly divided into 243 and 51 data sets for training and testing, respectively. The properties of the training and testing data sets for Model III are listed in Table 4.

3.2. Approach for developing ANFIS models

3.2.1. Clustering

The three ANFIS models were created in a similar manner within a MATLAB environment. For Model I, the eleven input parameters (OPC, SRPC, SF, S, FA, LF, sand, gravel, air, hybrid fibres and code of environmental exposure) were fuzzified after the implementation of an appropriate clustering method. Grid partitioning was not used due to the large number of input parameters that

would have led to an excessive number of rules. For instance, if two membership functions are assumed to describe the universe of discourse of the eleven input variables, a total of 2048 rules will be generated, which makes the calculations of the ANFIS network extremely slow and perhaps without convergence of the global error. Thus, subtractive clustering was used herein to initialize the three ANFIS models.

Clustering methods convert a universe of data into homogenous groups classified according to cluster centers from which the distance of data points are computed (Brown and Harris, 1994). This helps reducing the number of rules associated with an ANFIS model to describe the input-output behaviour of a given system. If the analyst does not have a clear decision on the number of clusters and their centers for a given set of data, subtractive clustering can be used to define this information. The general principle of this method assumes that each data point can act as a potential cluster center. Assuming (N) data points, the measure of potential (Pot_i) for an i^{th} data point is (Chiu 1994):

$$Pot_i = \sum_{j=1}^N e^{-\alpha \|x_i - x_j\|} \quad (1)$$

where ($\alpha = 4/r_a^2$) and (r_a) is the radius of cluster, (x_i and x_j) are data vectors in the data space including both input and output dimensions. A point with many neighbouring data points will have a high potential. After the potential of all data points is computed, the point with the highest potential is selected as the first cluster center. Then, to obtain a new cluster center, the potential of each point is updated by (Chiu 1994):

$$Pot_i = Pot_i - Pot_k e^{-\beta \|x_i - x_k\|} \quad (2)$$

where ($\beta = 4/r_b^2$) and $r_b = \eta * r_a$

(Pot_k) is the potential of the (k^{th}) cluster, (x_i) is the data point being subtracted and (x_k) is the k^{th} cluster center. The positive constant (r_b) is relatively greater than the radius of cluster (r_a) by the squash factor (η), which is a positive constant greater than 1 to avoid closely spaced cluster centers.

The acceptance of a cluster center based on the potential value is determined according to an acceptance threshold (ε) and rejection threshold (ε'). The process continues until all possible clusters in the input-output spaces are found. The number of clusters defines the number of membership functions in the input-output space. Subtractive clustering has four parameters (acceptance threshold (ε), rejection threshold (ε'), the radius of cluster (r_a), and the squash factor (η) affecting the resultant number of rules for an ANFIS model. In the present study, these values were selected as 0.5, 0.15, 0.5 and 1.25, respectively, for the three ANFIS models. These values led to small numbers of rules and satisfactory performance of the ANFIS models as will be shown later in the text.

3.2.2. Fuzzy inference method

There are several fuzzy inference methods, among which the Sugeno method is particularly effective for ANFIS models with given input-output data sets (Ross 2004). The Sugeno inference method was used in the present study to develop three ANFIS models for expansion, RE_d and TF since ANFIS models do not allow multiple outputs. An exemplar rule in a Sugeno model, which has two inputs (x and y) and an output (z) has the form:

$$R: \text{ IF } x \in A \text{ and } y \in B \quad \text{ THEN } z = f(x, y) \quad (3)$$

Where (A and B) are arbitrary fuzzy subsets in the antecedent, and $f(x, y)$ is a crisp function in the

consequent. When $f(x, y)$ is constant, the inference system is called zero-order Sugeno Model. If this function is linear, the inference model is called first-order Sugeno model. In a Sugeno model, each rule has a distinctive crisp output, i.e. rules are not allowed to share consequents, or the number of output membership functions equals the number of rules. The overall output (z) is obtained by a weighted average defuzzification method (Ross 2004):

$$z = \frac{\sum_{i=1}^n z_i \cdot w_i}{\sum_{i=1}^n w_i} \quad (4)$$

where (n) is the number of rules, (z_i) is the output of the i^{th} rule, and (w_i) is the weight (consequent) of the i^{th} rule.

3.2.3. Process

If a Gaussian membership function is selected to fuzzify the input variables, the shape of the membership function ($\mu(x)$) is described by (Ross 2004):

$$\mu(x) = e^{-\frac{1}{2} \left(\frac{x_i - c_i}{\sigma_i} \right)^2} \quad (5)$$

where (x_i) is the i^{th} input variable, and (c_i) and (σ_i) are parameters defining the shape of the curve of the input membership function (premise parameters). Applying a first-order Sugeno model for the two-input example in Eq. 3, the output for the i^{th} rule is given by:

$$z_i = a_i \cdot x_i + b_i \cdot y_i + c_i \quad (6)$$

where (a , b_i and c_i) represent the parameters defining the output side of the i^{th} rule (consequent parameters).

The ANFIS process starts by initializing the premise parameters using an appropriate clustering method (subtractive clustering was used in the present study), as previously explained. This is followed by forward computations for the consequent parameters using a least-square method. The RMSE between the experimental and predicted values should not exceed a target magnitude (a value of 1E-05 was implemented in this study). In a least-square algorithm, the linear system is expressed by (Jang, *et al.* 1997):

$$A\theta + \varepsilon = Y \quad (7)$$

where (ε) is an error value, (Y) is a target (known) output vector, (θ) is an unknown parameter vector and (A) is the design matrix defined by:

$$A = \begin{bmatrix} f_1(u) & \dots & f_n(u) \\ f_1(u_m) & \dots & f_n(u_m) \end{bmatrix} \quad (8)$$

in which, (u) is a known input vector and (f) defines known functions. This algorithm aims at finding the least-square estimator (θ) that minimizes the sum of squared error given by:

$$\|A\theta - Y\|^2 \quad (9)$$

To improve the learning process, the premise parameters are then updated using a back-

propagation technique (commonly used in artificial neural networks), in order to re-compute the new consequent parameters. In this technique, the convergence of a network is found by a least-square based energy function, and the network parameters are updated along its negative gradient (Haykin 1999) such that:

$$\delta_n = \frac{\partial E_n}{\partial v_n} \quad (10)$$

where (δ) is a local error gradient, (E) is an error energy function, (n) is the number of neurons in a layer and (v) is an induced local field given by:

$$v_n = \sum_{i=1}^m x_i w_i - b \quad (11)$$

in which, (x_i) is an input variable, (w_i) is a synaptic weight between connected neurons, (b) is a bias value and (m) is the number of neurons in a previous layer. The weight update (Δw) for a network layer with (n) number of neurons is expressed by:

$$\Delta w = \chi \delta_n Y_n \quad (12)$$

where (χ) is a learning parameter, and (Y) is an output vector. The output signal is calculated by an activation function that normalizes the local field (v) for the convergence of the network (Haykin 1999). Thus, the components of the fuzzy rules (premise and consequent parameters) in the rule-based engine are constantly changing at each training epoch until a minimum RMSE or desired number of epochs (500 in the present study) is reached. This hybrid (least-square and back-propagation methods) learning algorithm was used in the present study to train the three ANFIS models.

3.3. Models description

The purpose of Model I is to predict the expansion of SCC specimens exposed to different regimes of very severe sodium sulfate attack: full immersion, wetting-drying, freezing-thawing and cyclic cold-hot conditions without sustained flexural loading. Initially, subtractive clustering was applied to the 138 data sets in the training database. Subtractive clustering produced 84 fuzzy membership functions for the eleven (contents of OPC, SRPC, SF, S, FA, LF, sand, gravel, air, hybrid fibres and code of environmental exposure) input variables and consequently 84 rules in the rule-based engine were generated. The Gaussian (Eq. 5) membership function was selected, and first-order Sugeno model was adopted as the fuzzy inference method. In the rule-based engine, the fuzzified input variables were connected by T-norm (*logical “and”*) with a minimization operator. The supervised training of the model used hybrid least-square and back-propagation techniques to improve the learning process on 138 data points. Defuzzification of the output (expansion) was done by the weighted average method (Eq. 4). Training continued until a stable error decrement (after 196 epochs) was observed. The architecture of Model I is schematically illustrated in Fig. 1.

Model II was developed in a similar way to Model I. The purpose of this model is to predict RE_d of SCC specimens exposed to different regimes of very severe sodium sulfate attack: full immersion, wetting-drying, partial immersion, freezing-thawing and cyclic cold-hot conditions with and without sustained flexural loading. Subtractive clustering formed 105 Gaussian membership functions for the twelve (OPC, SRPC, SF, S, FA, LF, sand, gravel, air, hybrid fibres, code of environmental exposure and flexural stress ratio) input variables and 105 rules in the Sugeno rule-

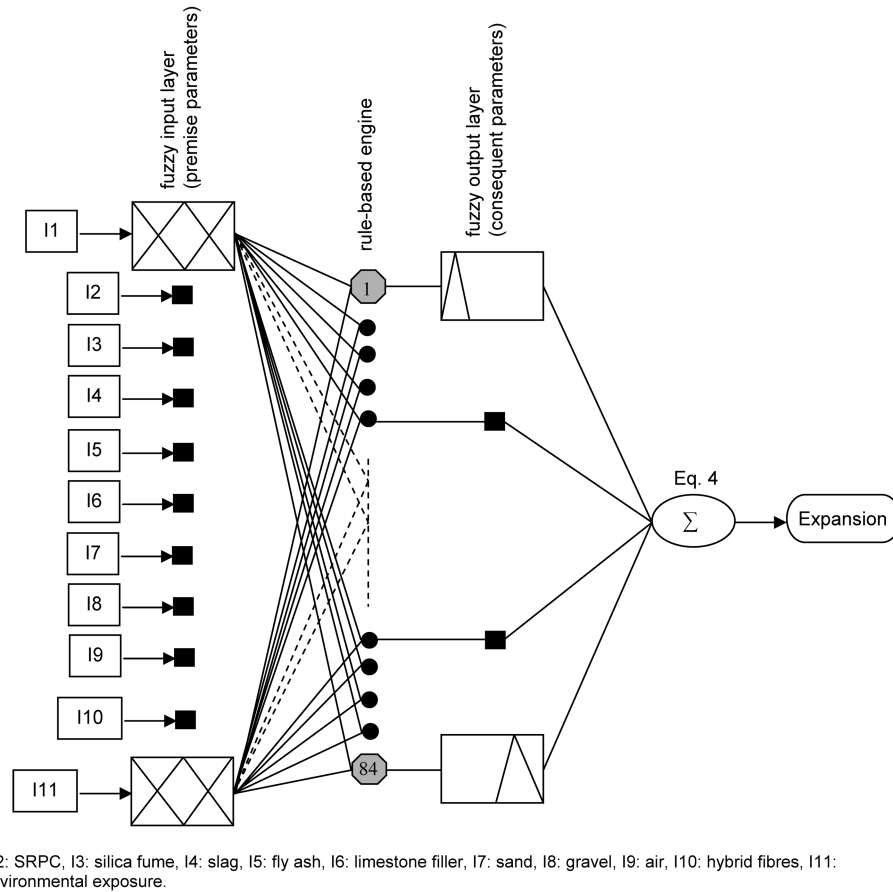


Fig. 1 Schematic diagram for ANFIS architecture of Model I

based engine. The used fuzzification, defuzzification and training methods were similar to that of Model I. Training was done using 244 data points, as explained in the database section, until a stable error decrement was reached (at 298 epochs). The architecture of Model II is similar to that of Model I (Fig. 1) except for the number of input variables (12), membership functions (105) and rules (105).

Model III was developed to predict *TF* of SCC under various high-concentration sodium sulfate exposure regimes from the twelve input parameters used in Model II. Subtractive clustering produced 109 Gaussian membership functions for the input variables and 109 rules in the Sugeno rule-based engine. The fuzzification, defuzzification and training methods were similar to that of models I and II. The training process was conducted on 243 data points until a stable error decrement was reached (at 303 epochs). The architecture of Model III is similar to that of Model I (Fig. 1) except for the number of input variables (12), membership functions (109) and rules (109).

4. Results and discussion

The performance of ANFIS models depends on the success of the training process. Successful

ANFIS models should give accurate output predictions not only for input data used in the training process, but also for new testing data unfamiliar to the trained models. At the training stage, the performance of the three ANFIS models was assessed based on the average absolute error (*AAE*) and the ratio of experimental-to-predicted property according to the following equations, respectively:

$$AAE = \frac{1}{n} \sum \frac{|P_{exp} - P_{pre}|}{P_{exp}} \times 100 \quad (13)$$

$$\frac{P_{exp}}{P_{pre}} \quad (14)$$

where (P_{exp}) and (P_{pre}) are the experimental and predicted properties (expansion, RE_d or TF), respectively, and (n) is the number of data points.

For Model I, satisfactory completion of the training process was verified by requiring the ANFIS model to predict the expansion of the SCC specimens from the training data set using the eleven input variables, and the predictions are shown in Fig. 2a. It can be noted that the ANFIS model has captured the input-output relationships since the points are mostly located on or slightly under/above the equity line between the experimental and predicted expansion values. The *AAE*, average P_{exp}/P_{pre} and the coefficient of variation (COV) of P_{exp}/P_{pre} of the training data points were 3.28%, 1.00 and 5.33%, respectively, which indicates that the performance of Model I is satisfactory.

To examine the generalization capacity of Model I, it was tested on 30 data points (testing data), randomly selected from the total 168 data points. Such testing points were not previously shown to

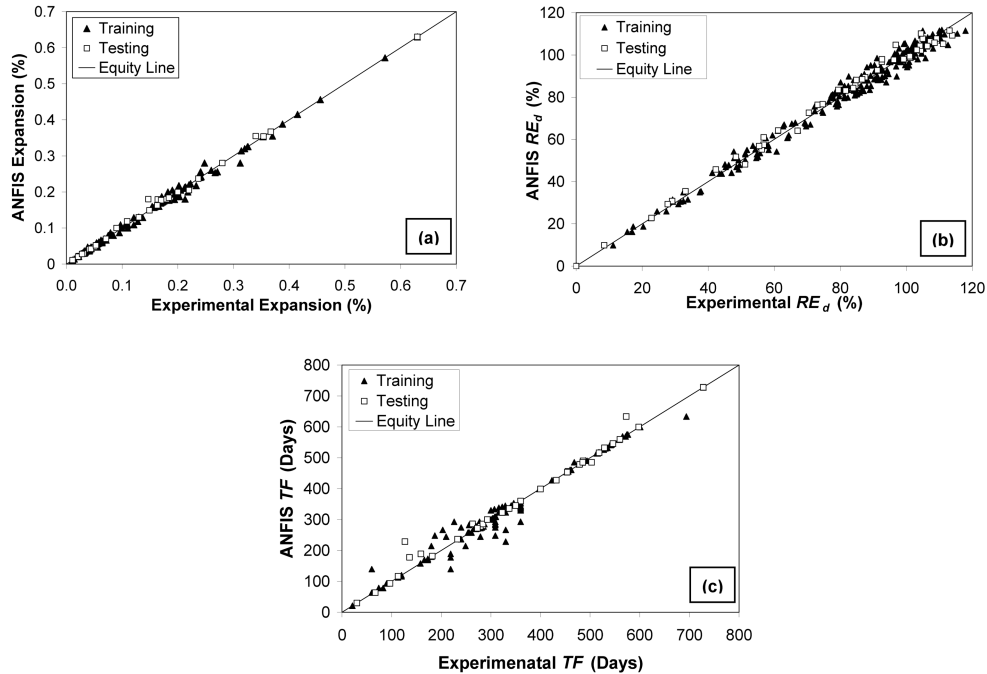


Fig. 2 Response of ANFIS models in predicting: (a) expansion, (b) RE_d , and (c) TF values of SCC specimens exposed to various sulfate attack regimes

Table 5 Performance of models I, II and III

Model/Property	Training Data				Testing Data			
	AAE (%)	P_{exp}/P_{pr}			AAE (%)	P_{exp}/P_{pre}		
		Average	STDEV	COV		Average	STDEV	COV
I/Expansion (%)	3.28	1.00	0.05	5.33	2.92	0.99	0.05	5.08
II/ RE_d (%)	3.03	1.00	0.04	3.92	3.23	0.99	0.04	3.94
III/ TF (Days)	2.76	1.00	0.08	7.83	3.47	0.98	0.08	7.68

the model, and thus the predictive capacity of the model for new unknown data can be evaluated. The eleven input parameters of the testing data points were introduced to Model I and the response (predicted expansion values of SCC specimens) are shown in Fig. 2a. Similar to the case with the training data points, Model I showed good predictions relative to the actual experimental data, and testing data points in Fig. 2a were mostly located on or slightly deviated from the equity line. The *AAE*, average P_{exp}/P_{pre} and COV of P_{exp}/P_{pre} of the testing data points were 2.92%, 0.99 and 5.08%, respectively. Hence, it can be deduced that Model I has a satisfactory generalization capacity for predicting the expansion values of similar SCC specimens exposed to various high-concentration sodium sulfate exposure regimes: full immersion, wetting-drying, freezing-thawing and cyclic cold-hot conditions without sustained flexural loading. Table 5 summarizes the statistical parameters for the response of Model I to the training and testing data.

Model II was developed to predict the decline in the elastic dynamic modulus (RE_d) of SCC specimens under different high-concentration sodium sulfate exposure regimes (full immersion, wetting-drying, partial immersion, freezing-thawing, and cyclic cold-hot conditions with or without flexural loading) based on 12 input parameters. The response of Model II relative to the experimental RE_d values for the 244 training and 50 testing data sets is illustrated in Fig. 2b. It can be observed that most training and testing data points lay on or in the vicinity of the equity line, indicating a good agreement between the predicted and experimental RE_d values. The statistical parameters for Model II predictions of both training and testing data are summarized in Table 5. Successful training of Model II (*AAE* of 3.03%) led to a good generalization capacity. The *AAE*, average P_{exp}/P_{pre} and COV of P_{exp}/P_{pre} of the testing data points were 3.23%, 0.99 and 3.94%, respectively. Thereby, Model II can effectively predict the RE_d of similar SCC specimens exposed to high-concentration sodium sulfate attack under various environmental and flexural loading conditions.

Model III was developed to predict the onset of failure (TF) for the SCC specimens exposed to very severe sodium sulfate attack under different environmental and flexural loading conditions. The response of Model III for the 243 training and 51 testing data points is shown in Fig. 2c. In this figure, several data points lay on top of each other due to similar TF . Also, it can be observed that few points are relatively scattered away from the equity line. These points are from the very severe sodium sulfate exposure involving cyclic cold-hot conditions with flexural loading which showed variability in the TF of replicate SCC specimens. For instance, under cyclic cold-hot environments and 0.25 flexural stress ratio, two replicates from the ternary (B3-A-40) SCC mixture broke at 226 and 360 days, respectively. In such a case, the ANFIS model reasonably introduced an average (i. e. 293 days) approximation between the two values. This gives a relatively high (average of 24.64%) *AAE* for both data points. Nevertheless, the overall performance of Model III was satisfactory for both the training and testing phases. The overall *AAE* for the training stage was 2.76%. Also, a

satisfactory generalization capacity for Model III was ensured from the AAE, average P_{exp}/P_{pre} and COV of P_{exp}/P_{pre} of the testing data points which were 3.47%, 0.98 and 7.68%, respectively. The statistical parameters of the response of Model III are listed in Table 5.

5. Sensitivity analyses

Models I, II and III showed satisfactory performance and demonstrated their ability to predict expansion, RE_d and TF , respectively, for a wide range of SCC mixture designs under various high-concentration sodium sulfate exposure regimes. The purpose of this section is to investigate the ability of these models to capture the sensitivity of the predicted properties to individual input parameters. The sensitivity analysis was done by randomly selecting a single SCC mixture from Table 2 (base mixture) to create multiple new mixtures (not previously shown to the models) with various levels (within the range of training data) of the parameter of interest. Other input variables remained constant or slightly changed (mostly the sand content) according to the absolute volume mixture design method. The selected parameters of interest were the level of SCMs in quaternary binders without limestone filler, air content, S/A, volume of hybrid fibres and flexural stress ratio.

5.1. Sensitivity to level of supplementary cementitious materials (SCMs)

The sensitivity of the three ANFIS models to the level of SCMs in quaternary binders without limestone filler was investigated using the parameters summarized in Table 6. For the created mixtures, the mass ratio of SF: S: FA was 1: 5: 4, and the total cementitious content was 470 kg/m³ similar to the base mixture. It is worth noting that the chosen environmental exposure (wetting-drying) promoted salt crystallization in addition to sodium sulfate attack reactions. MIP and SEM microanalyses showed that cementitious matrices made from quaternary binders with SCM dosages of up to 50% had a very fine pore structure that was vulnerable to damage by salt crystallization. This was clearly captured by the three ANFIS models, which showed adverse effects (high

Table 6 Parameters used in the sensitivity analysis

Section	Input Variable	Base Mixture	Levels of Input Variable	Sulfate Attack Exposure Regime	Sustained Flexural Loading
5.1	Level of SCMs (SF+S+FA)	A5-N-50	5, 10, 20, 30, 40, and 50%	Wetting-Drying	--
5.2	Air Content	A4-N-50	1.5, 2.5, 3.5, 4.5, 5.5, 6.5, and 7%	Cyclic Cold-Hot Conditions	--
5.3	Sand-to-Aggregate Mass Ratio	B1-A-40	40, 43, 46, 50, 55, and 60%	Wetting-Drying	
5.4	Volume of Hybrid Fibres	C5-A-H	0.05, 0.10, 0.20, 0.30, 0.40, and 0.47%	Freezing-Thawing	
5.5	Flexural Stress Ratio	A5-N-50	0, 0.10, 0.20, 0.30, 0.40, 0.45, and 0.50	Cyclic Cold-Hot Conditions	0 to 50% of the Flexural Strength

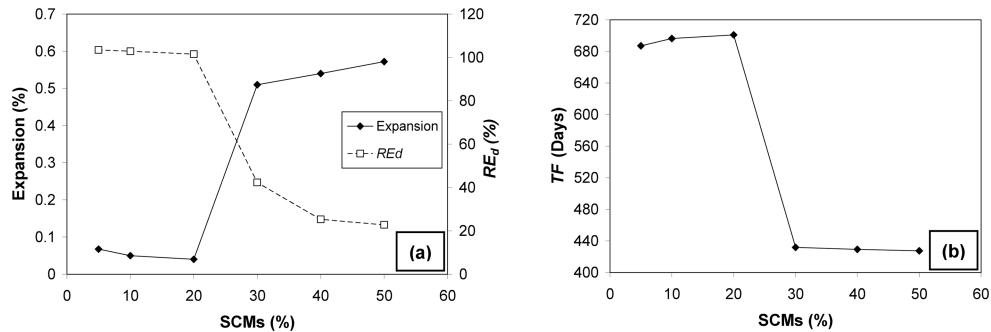


Fig. 3 Sensitivity of ANFIS models to the dosage of SCMs in quaternary binders without limestone filler in predicting: (a) expansion and RE_d , and (b) TF values under the wetting-drying exposure (period of testing was 728 days)

expansion, low RE_d and early TF -Fig. 3) for the mixtures with SCM (SF + S + FA) dosages around 30% and higher. Extreme pore size refinement, due to higher dosages of SCMs, renders such cementitious matrices subject to intensive micro-cracking in the case of salt crystallization. This is similar to the well-documented salt weathering of rocks having very fine pore structure.

5.2. Sensitivity to air content

To investigate the sensitivity of the ANFIS models to variation in the air content, the parameters summarized in Table 6 were used. Figs. 4a-b show the ANFIS models predictions of expansion and RE_d and TF , respectively. It can be noted that the models were sensitive to the transition from non-air-entrained to air-entrained cementitious matrices. Air-entrained specimens (air contents above about 4%) had lower expansion, higher RE_d and almost double TF relative to the corresponding non-air-entrained specimens. Such a trend complied with microscopy studies. SEM micrographs showed that the existence of well dispersed network of air bubbles (air-entrainment) that accommodated the nucleation and growth of crystalline phases (gypsum, ettringite, thaumasite, and mirabilite) in the cementitious matrix due to such an exposure (very severe sodium sulfate attack with cyclic cold-hot conditions). Also, air bubbles acted as a relief mechanism for osmotic and

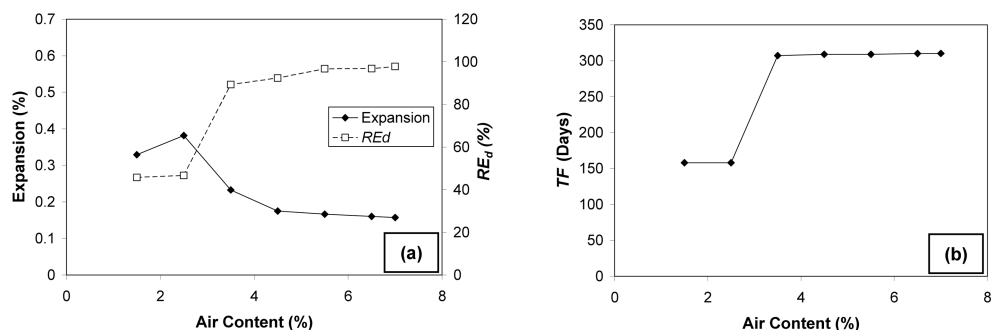


Fig. 4 Sensitivity of ANFIS models to the air content of quaternary binders with limestone filler in predicting: (a) expansion and RE_d , and (b) TF values under the cyclic cold-hot conditions without sustained flexural loading (period of testing was 365 days)

hydraulic pressures developed within the cementitious matrices. This generally caused lower and/or delayed damage, which led to the longevity of air-entrained SCC specimens made with all cementitious binders.

5.3. Sensitivity to Sand-to-aggregate mass ratio

To test the sensitivity of the ANFIS models to variation in the sand-to-aggregate mass ratio (S/A), the parameters summarized in Table 6 were used. Figs. 5a-b show that the predictions of the three ANFIS models were relatively insensitive to variations in S/A between 40-60%. The expansion, RE_d and TF had comparable values without a definite trend. This complies with thermal, mineralogical and micro-analytical studies which showed that the degradation of SCC specimens under all sodium sulfate attack exposure regimes was mainly controlled by other factors such as the volume of cementitious paste, type of binder and air-entrainment. Also, analysis of variance confirmed the insensitivity of experimental results to variation of S/A from 40 to 60%.

5.4. Sensitivity to volume of hybrid fibres

To test the sensitivity of the ANFIS models to the volume of hybrid fibres, the parameters summarized in Table 6 were used. The designated exposure regime was high-concentration sodium sulfate attack combined with freezing-thawing cycles. The responses of the three models indicated

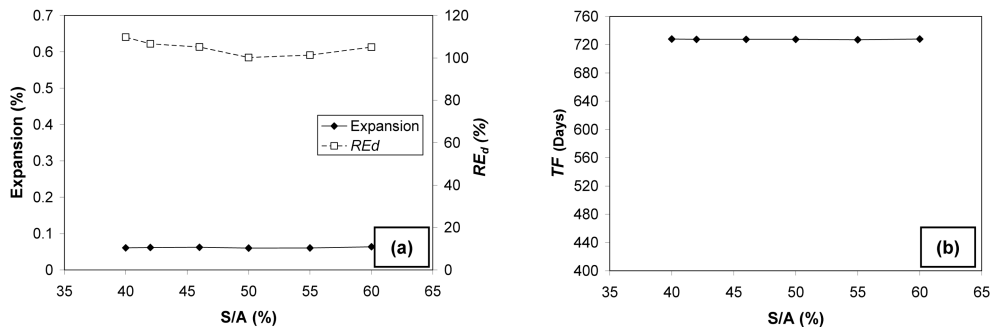


Fig. 5 Sensitivity of ANFIS models to the S/A of control binders in predicting: (a) expansion and RE_d , and (b) TF values under the wetting-drying exposure (period of testing was 728 days)

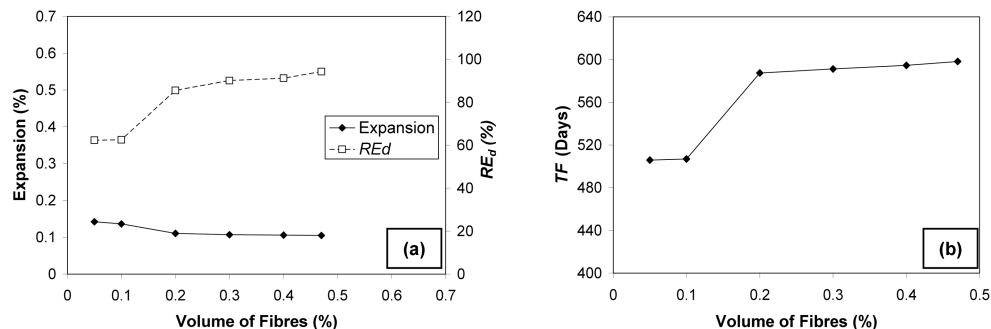


Fig. 6 Sensitivity of ANFIS models to the volume of fibres of quaternary binders in predicting: (a) expansion and RE_d , and (b) TF values under the freezing-thawing exposure (period of testing was 605 days)

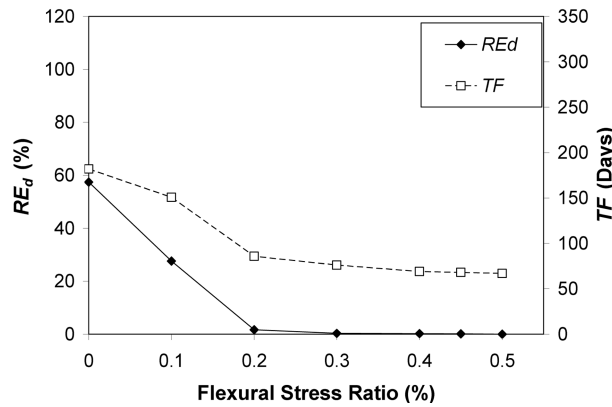


Fig. 7 Sensitivity of ANFIS models to applied flexural stress ratio under cyclic cold-hot conditions combined with sulfate attack

that as the volume of hybrid fibres increased from 0.05 to 0.47%, the durability of the SCC specimens significantly improved (Fig. 6). This was exhibited by 26% reduction in expansion, an increase in RE_d beyond 90% (Fig. 6a) and a delay of TF by more than 100 days (Fig. 6b). This agrees with experimental observations, where SCC specimens comprising hybrid fibre reinforcement sustained a higher (610) number of freezing-thawing cycles (combined with sodium sulfate attack) without drastic damage. This was attributed to the significant effect of micro- and macro-fibres in controlling cracking of cementitious matrices, and thus limiting the rate of damage.

5.5. Sensitivity to flexural stress ratio

The parameters listed in Table 6 were used to examine the effect of variation in the flexural stress ratio on the responses of the ANFIS models. The results are shown in Fig. 7. The ANFIS models indicate that as the flexural loading level increases beyond 0.25, breakage (zero RE_d) of specimens can occur at early TF (within only 80 days of exposure). The damage rate is substantially accelerated at a higher load level (Fig. 7). This agrees with experimental observations which showed that the SCC specimens substantially deteriorated (low RE_d and high expansion values) under such an exposure (combined high-concentration sodium sulfate and consecutive cold-hot conditions). The situation was much worsened with concurrent application of sustained flexural stress due to the additional effect of stress corrosion, which led to more frequent breakage of specimens with increasing applied flexural stress ratio from 0.25 to 0.5. In addition, under this exposure regime, thermal, mineralogical and micro-analytical studies showed that sulfate reaction products formed at relatively deeper regions (from the tension surface) in the SCC specimens due to the direct penetrability of the sodium sulfate solution through flexural micro-cracks.

6. Effect of environmental conditions

From the experimental database and predictions of the ANFIS models, it can be noted that the environmental exposure accompanying very severe sodium sulfate attack had a pronounced effect on the degree of deterioration of the SCC specimens. Fig. 8, which depicts the average time of

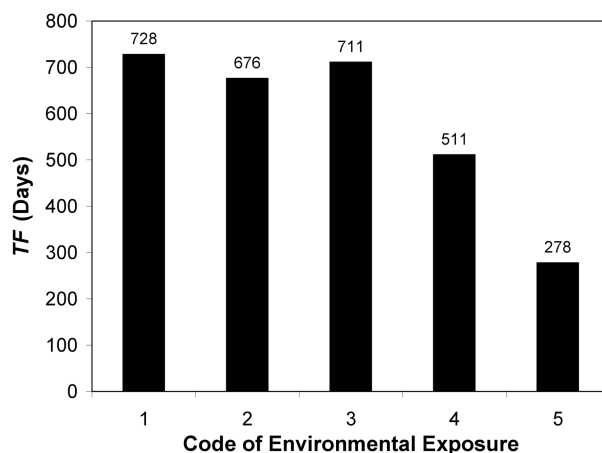


Fig. 8 Average time to failure of the SCC specimens under the five sulfate attack exposure regimes

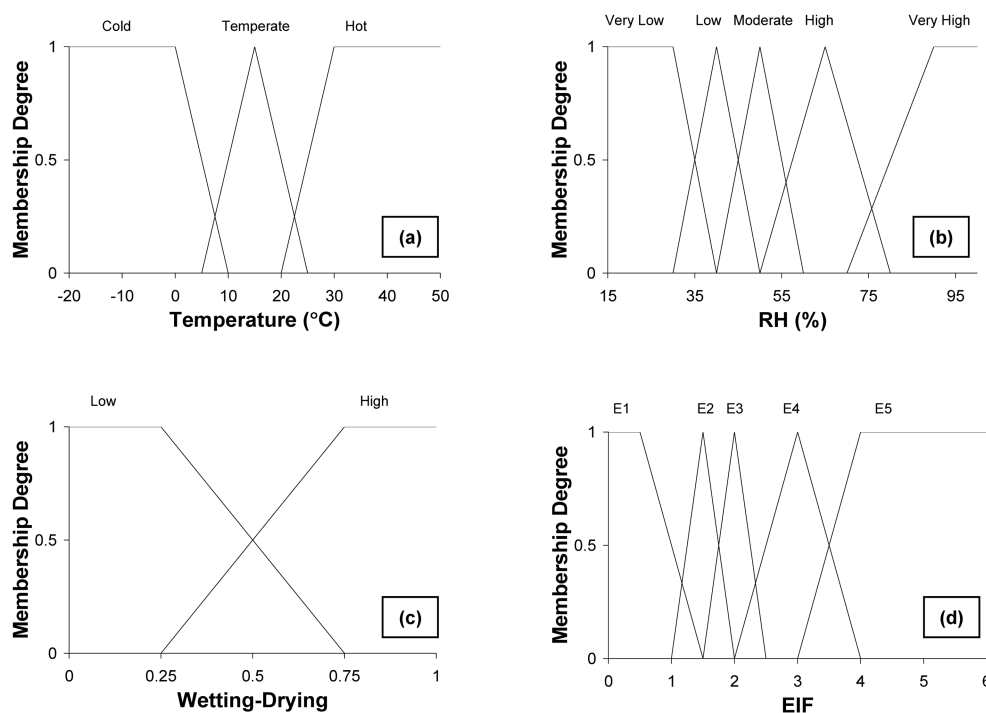


Fig. 9 Membership functions for the input and output parameters of the environmental fuzzy inference system: (a) temperature, (b) RH, (c) wetting-drying, and (d) EIF

failure of the tested SCC specimens in each exposure regime, substantiates this observation. Exposure 1 (full immersion) was the least aggressive (TF of 728 days) relative to the other exposures, while exposure 5 (consecutive cold-hot conditions), which represents seasonal climatic conditions in various geographic locations, was the most aggressive (TF of 278 days).

Fuzzy inference methods can be used to determine the severity of environmental conditions accompanying an aggressive (more than 10,000 ppm) sodium sulfate solution. Based on the average

Table 7 Environmental fuzzy inference system for sulfate attack

Description of Exposure	Temperature (°C)	RH(%)	Wetting-Drying	EIF
Full Immersion	20.0	100	0	1.50
Wetting-Drying	32.0	72	1.0	3.00
Partial Immersion	32.0	57	0.5	2.78
Freezing-Thawing	6.5	88	0.2	4.25
Cyclic Cold-Hot Cold conditions	-10.5	93	0	4.85
Hot	30.0	68	1.0	3.20

Table 8 Rule-based engine for the environmental fuzzy inference system at low and high levels of wetting-drying

Temperature \ RH	Very Low	Low	Moderate	High	Very High
Low Level of Wetting-Drying					
Cold	E1	E1	E2	E4	E5
Temperate	E1	E1	E2	E2	E2
Hot	E2	E3	E3	E4	E4
High Level of Wetting-Drying					
Cold	E2	E2	E3	E5	E5
Temperate	E3	E3	E3	E2	E2
Hot	E4	E4	E4	E4	E4

temperature, relative humidity and degree of wetting-drying, an environmental impact factor (EIF) can be predicted. Hence, a fuzzy inference system was constructed to estimate the EIF of the five sodium sulfate attack exposure regimes implemented in the present study.

To account for uncertainty in the input parameters (temperature, relative humidity and degree of wetting-drying), fuzzy sets were constructed using respective triangular membership functions, as illustrated in Fig. 9a-c. The crisp values of the input variables of the five exposure regimes are listed in Table 7. The fuzzy output of this FIS, shown in Fig. 9d, is an EIF which reflects the severity of environmental conditions associated with a high-concentration sodium sulfate solution. The rule-based engine of the FIS is the link between the input variables and EIF. It reflects engineering experience regarding the deterioration of SCC under various high-concentration sodium sulfate exposure regimes. Thirty rules were constructed in the form of IF-THEN statements comprising linguistic antecedents and consequents. Table 8 outlines these rules in a matrix format. The T-norm “logical and” was used to connect antecedents and implied a minimization “min” operator. The Mamdani-type inference system was used with a minimization implication operator for individual consequents of each rule. The Sugeno-type was not used since it does not allow rules to share similar fuzzy outputs (consequents). After aggregation of the consequents of each rule by maximization, the centroid method (similar to Eq. 4) was applied for defuzzification of the EIF fuzzy output, and the results are listed in Table 7.

The EIF results had a scale of 0-6, which corresponds to ‘negligible’ to ‘extremely severe’ environmental aggression accompanying a high-concentration sodium sulfate solution. The EIF results in Table 7 complied with experimental observations. The reference (full immersion) exposure

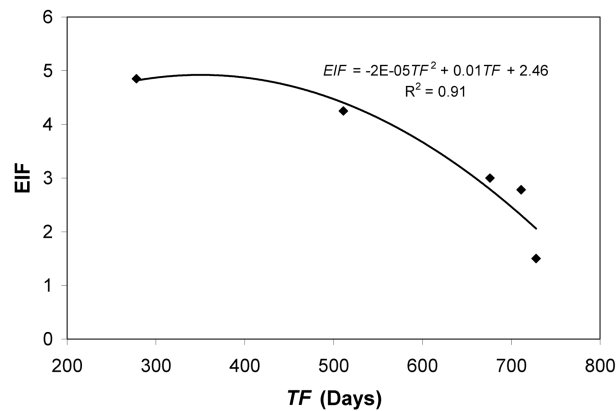


Fig. 10 Time to failure of SCC specimens versus predicted EIF

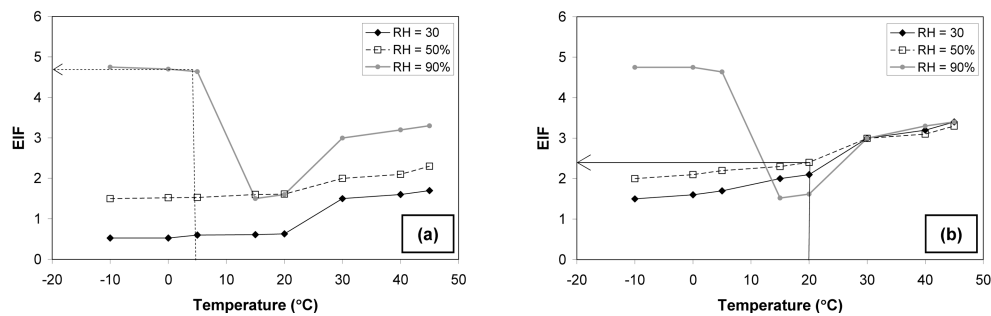


Fig. 11 EIF associated with severe sulfate attack at: (a) low, and (b) high levels of wetting-drying

had the least EIF of 1.50 (i.e. the least aggressive sodium sulfate attack exposure), while the consecutive cold-hot conditions (exposure 5), had the highest EIF ranging between 4.85 and 3.20. The exposure of very severe sodium sulfate attack coupled with freezing-thawing cycles also had a high EIF (4.25) in agreement with experimental observations. Overall, the EIF results of the five exposure regimes correlated well with their corresponding average TF values (quadratic function ($R^2 = 0.91$)-Fig. 10). Hence, environmental charts of very severe sodium sulfate attack (Figs. 11a-b) were developed from the constructed fuzzy inference system under low and high levels of wetting-drying. Such charts can be used to predict the severity of environmental conditions associated with a high-concentration sodium sulfate attack based on the expected average temperatures, relative humidity and degree of wetting-drying.

To clarify the use of those environmental charts, two examples are presented. If a shallow foundation is embedded in a saturated soil (low level of wetting-drying) with a sodium sulfate concentration in the groundwater of more than 10,000 ppm, and the prevailing climatic conditions are cold and humid (average annual temperature and RH of 5°C and 90%, respectively), an EIF of 4.64 is obtained using Fig. 11a. This represents a very severe environmental effect accompanying sodium sulfate attack, where accelerated deterioration of the cementitious matrix is most likely to occur. Comparatively, if a pavement is in contact with a saturated soil having a sodium sulfate concentration in the groundwater of more than 10,000 ppm, and the prevailing climatic conditions are temperate with several cycles of rainfall (high level of wetting-drying) throughout the year, an EIF of 2.40 is obtained using Fig. 11b. This represents a moderate environmental aggression

accompanying sodium sulfate attack, suggesting a slower degradation of the cementitious system. Overall, a low EIF implies a long service life with less frequent maintenance of concrete and vice versa for a high EIF.

7. Conclusions

The present study showed that adaptive neuro-fuzzy inference systems (ANFIS) can be used to predict the behaviour of cement-based materials under various exposure regimes of very severe sodium sulfate attack. Such models combine the advantages of artificial neural networks (e.g. self-learning and pattern recognition) and fuzzy inference systems (e.g. accommodating uncertainty, linguistic use and approximation). Based on the results obtained in the present study, the following conclusions can be drawn:

- Predicting the behaviour of SCC under very severe sodium sulfate attack based on mixture ingredients, environmental exposure and level of flexural loading involves ambiguous/unknown interrelationships, uncertainty and non-linearity. Thus, an analytical model may be extremely complicated and would inevitably include oversimplifying assumptions. On the contrary, well-trained ANFIS models can accommodate all of these factors and give relatively accurate predictions for complex durability issues such as sulfate attack of concrete under field-like exposure.
- The three ANFIS models developed in the present study accurately predicted the behaviour (expansion, RE_d , and TF) of a wide range of self-consolidating concrete (SCC) mixture designs under various exposure regimes of high-concentration sodium sulfate attack. The models had a good generalization capacity beyond the training stage as verified by results obtained on new testing data within the range of training database.
- Sensitivity analysis showed that the developed models captured the effect of individual input parameters on the results. Thus, these models could be used to forecast the deterioration of tailor-made SCC mixture designs exposed to high-concentration sodium sulfate attack combined with various environmental and flexural loading conditions. In the design and prequalification stage of a construction project, such models can reduce the need for exhaustive trial batches and long-term experimental programs, thus facilitating the decision-making process.
- The developed ANFIS models are versatile and can be re-trained to encompass wider ranges of input variables, different concentrations of sodium sulfate solutions, other types of sulfate solutions, other environmental conditions, etc. However, there is dearth of information on the behaviour of concrete under sulfate attack combined with various environmental conditions and/or structural loading. Once, this data becomes available in the future, the re-training process of these models would be readily achievable.
- Due to the importance of the effect of environmental conditions on sodium sulfate attack degradation mechanisms, a fuzzy inference system was developed to predict an environmental impact factor (EIF). Based on the average temperature, relative humidity and degree of wetting-drying, environmental charts for severe sodium sulfate attack were constructed. This can assist designers/quality control personnel in determining the degree of severity of a certain environmental exposure associated with sodium sulfate attack, and thus identifying optimum concrete mixtures, preventive measures, maintenance schedules, etc.
- Similar to the ANFIS models, the environmental fuzzy inference system model is versatile and

can be easily updated/modified according to future findings in the area of sulfate attack of concrete under various environmental exposure regimes.

Acknowledgements

A grant provided by the Natural Science and Engineering Research Council of Canada (NSERC) for manufacturing a state-of-the-art walk-in environmental chamber used in this research is highly appreciated. The continued financial support of NSERC through a discovery grant to M. Nehdi is highly acknowledged. Funding of the Ontario Innovation Trust (OIT) and the Canada Foundation for Innovation (CFI) that allowed creating a state-of-the-art laboratory has been crucial to this research. M. T. Bassuoni is indebted to the Ontario Graduate Scholarship (OGS) and the University of Western Ontario (UWO) for supporting his doctoral studies.

References

- ACI Committee 237. (2007), *Self-Consolidating Concrete* (237R-07), American Concrete Institute, Farmington Hills, MI, USA, 30p.
- Al-Amoudi, O.S.B. (2002), "Attack on plain and blended cements exposed to aggressive sulfate environments", *Cement Concrete Comp.*, **24**(3-4), 305-316.
- Bassuoni, M.T. (2008), *Integrated Approach for Investigating the Durability of Self-consolidating Concrete to Sulfate Attack*, PhD Dissertation, University of Western Ontario, Canada, 402p.
- Boel, V., Audenaert, K., De Schutter, G., Heirman, G., Vandewalle, L., Desmet, B., and Vantomme, J. (2007), "Transport properties of self compacting concrete with limestone filler and fly ash", *Mater. Struct.*, **40**(5), 507-516.
- Anoop, M.B., Rao, K.B., and Rao, T.V. (2002), "Application of fuzzy sets for estimating service life of reinforced concrete structural members in corrosive environments", *Eng. Struct.*, **24**(9), 1229-1242.
- ASTM C 1012, (2004), "Standard test method for length change of hydraulic-cement mortar exposed to a sulfate solution", *Annual Book of American Society for Testing Materials*, V. 4.01, West Conshohocken, PA.
- ASTM C 215, (2004), "Standard test method for fundamental transverse, longitudinal, and torsional resonant frequencies of concrete specimens", *Annual Book of American Society for Testing Materials*, V. 4.02, West Conshohocken, PA.
- ASTM C 666, (2004), "Standard test method for resistance of concrete to rapid freezing and thawing", *Annual Book of American Society for Testing Materials*, V. 4.02, West Conshohocken, PA.
- Bentz, D., Ehlen, M., Ferraris, C., and Garboczi, E. (2001), "Sorptivity-based service life predictions for concrete pavements", *Proceedings of 7th International Conference on Concrete Pavements*, Orlando, Florida, USA, V. 1, pp. 181-193.
- Brown, M. and Harris, C. (1994), *Neurofuzzy Adaptive Modelling and Control*, Prentice Hall, NY, USA, 508p.
- Brown, P. and Taylor, H. (1999), "The role of ettringite in external sulfate attack", In: J. Marchand and J. Skalny (eds.) *Materials Science of Concrete Special Volume: Sulfate Attack Mechanisms*, The American Ceramic Society, pp. 73-98.
- Chiu, S. (1994), "Fuzzy model identification based on cluster estimation", *J. Intelligent. Fuzzy Sys.*, **2**(3), 267-278.
- Cohen, M. and Mather, B. (1991), "Sulfate attack on concrete-research needs", *ACI Mater. J.*, **88**(1), 62-69.
- De Schutter G. Audenaert K (eds), (2007), *Durability of self-compacting concrete*, State-of-the-Art Report of RILEM Technical Committee 205-DSC, RILEM Report 38, RILEM Publications S.A.R.L., 185p.
- Do, J. (2006), "Fuzzy inference based cover thickness estimation of reinforced concrete structure quantitatively considering salty environment impact", *Comput. Concrete*, **3**(2/3), 145-161.
- Do, J., Song, H., So, S., and Soh, Y. (2005), "Fuzzy methodology application for modeling uncertainties in chloride

- ingress models of rc building structure”, *Comput. Concrete*, **2**(4), 325-343.
- El-Chabib, H. and Nehdi, M. (2005), “Neural network modelling of properties of cement-based materials demystified”, *Advances in Cement Res.*, **17**(3), 91-102.
- Ferraris, C., Stutzman, P., and Snyder, K. (2006), “Sulfate resistance of concrete: a new approach”, PCA R & D No. 2486, Portland Cement Association, Skokie, IL, 78p.
- Göktepe, A., İnan, G., Ramyar, K., and Sezer, A. (2006), “Estimation of sulfate expansion of PC mortar using statistical and neural approaches”, *Constr. Build. Mater.*, **20**(7), 441-449.
- Haj-Ali, R., Kurtis, K., and Sthapit, A. (2001), “Neural network modeling of concrete expansion during long-term sulfate exposure”, *ACI Mater. J.*, **98**(1), 36-43.
- Haykin, S. (1999), *Neural Networks: A Comprehensive Foundation*, Prentice Hall, NJ, USA, 842p.
- Hewlett, P.C., (1998), *Lea's Chemistry of Cement and Concrete*, Arnold, UK, 1053p.
- İnan, G., Göktepe, A., Ramyar, K., and Sezer, A. (2007), “Prediction of sulfate expansion of PC mortar using adaptive neuro-fuzzy methodology”, *Build. Environ.*, **42**(3), 1264-1269.
- Jang, J., Sun, C., and Mizutani, E. (1997), *Neuro-Fuzzy and Soft Computing*, Prentice Hall, N. J., USA, 614p.
- Kawamura, K. and Miyamoto, A. (2003), “Condition state evaluation of existing reinforced concrete bridges using neuro-fuzzy hybrid system”, *Comput. Struct.*, **81**(18-19), 1931-1940.
- Kim, Y., Kim, C., and Hong, S. (2006), “Fuzzy based state assessment for reinforced concrete building structures”, *Eng. Struct.*, **28**(9), 1286-1297.
- Marchand, J. (2001), “Modelling the behaviour of unsaturated cement systems exposed to aggressive chemical environments”, *Mater. Struct.*, **34**(4), 195-200.
- Mehta, P.K. (2000), “Sulfate attack on concrete: separating myths from reality”, *Concrete Int.*, **22**(8), 57-61.
- Ming-yu, H. and Ming-shu, T. (2006), “Use of fuzzy neural network to evaluate effect of composition of fly ash in suppressing AAR”, *ACI Mater. J.*, **103**(3), 161-168.
- Neville, A. (2004), “The confused world of sulfate attack on concrete”, *Cement Concrete Res.*, **34**(8), 1275-1296.
- Ross, T. (2004), *Fuzzy logic with engineering applications*, John Wiley & Sons, UK, 628p.
- Samson, E. and Marchand, J. (2007), “Modeling the transport of ions in unsaturated cement-based materials”, *Comput. Struct.*, **85**(23-24), 1740-1756.
- Skalny, J. and Pierce, J. (1999), “Sulfate attack: An Overview”, In: J. Marchand and J. Skalny (eds.) *Materials Science of Concrete Special Volume: Sulfate Attack Mechanisms*, The American Ceramic Society, pp. 49-63.
- Skalny, J., Marchand, J., and Odler, I. (2002), *Sulfate Attack on Concrete*, Spon Press, UK, 217p.
- Zhu, W. and Bartos, J. (2003), “Permeation properties of self-compacting concrete”, *Cement Concrete Res.*, **33**(6), 921-926.